OPEN

Positron Emission Tomography scanning in Anti-Neutrophil Cytoplasmic Antibodies-Associated Vasculitis

Michael J. Kemna, BSc, Frédéric Vandergheynst, MD, Stefan Vöö, MD, PhD, Didier Blocklet, MD, Thomas Nguyen, MD, Sjoerd A.M.E.G. Timmermans, BSc, Pieter van Paassen, MD, PhD, Elie Cogan, MD, PhD, Marinus J.P.G. van Kroonenburgh, MD, PhD, and Jan Willem Cohen Tervaert, MD, PhD

Abstract: Tools for evaluation of disease activity in patients with anti-neutrophil cytoplasmic antibodies (ANCA)-associated vasculitis (AAV) include scoring clinical manifestations, determination of biochemical parameters of inflammation, and obtaining tissue biopsies. These tools, however, are sometimes inconclusive. 2-deoxy-2-[^{18}F]-fluoro-D-glucose (FDG) positron emission tomography (PET) scans are commonly used to detect inflammatory or malignant lesions. Our objective is to explore the ability of PET scanning to assess the extent of disease activity in patients with AAV.

Consecutive PET scans made between December 2006 and March 2014 in Maastricht (MUMC) and between July 2008 and June 2013 in Brussels (EUH) to assess disease activity in patients with AAV were retrospectively included. Scans were re-examined and quantitatively scored using maximum standard uptake values (SUVmax). PET findings were compared with C-reactive protein (CRP) and ANCA positivity at the time of scanning.

Forty-four scans were performed in 33 patients during a period of suspected active disease. All but 2 scans showed PET-positive sites, most commonly the nasopharynx (n = 22) and the lung (n = 22). Forty-one clinically occult lesions were found, including the thyroid gland (n = 4 patients), aorta (n = 8), and bone marrow (n = 7). The amount of hotspots, but not the highest observed SUVmax value, was higher if CRP levels were elevated. Seventeen follow-up scans were made in 13 patients and showed decreased SUVmax values.

FDG PET scans in AAV patients with active disease show positive findings in multiple sites of the body even when biochemical parameters are inconclusive, including sites clinically unsuspected and difficult to assess otherwise.

Editor: Michael Masoomi.
Received: December 26, 2014; revised: March 12, 2015; accepted: March 14, 2015.
From the Clinical and Experimental Immunology, Maastricht University Medical Center (MJK, SAMEGT, PP); Cardiovascular Research Institute Maastricht (CARIM), Maastricht University, Maastricht, The Netherlands (MJK, SAMEGT, JWCT); Department of Internal Medicine, Erasme University Hospital, Université Libre de Bruxelles, Brussels, Belgium (FV, TN, EC); Department of Nuclear Medicine, Maastricht University Medical Centre, Maastricht, The Netherlands (SV, MJPGVK); Department of Nuclear Medicine, Erasme University Hospital, Université Libre de Bruxelles, Brussels, Belgium (DB); Clinical and Experimental Immunology, Maastricht University, Maastricht (JWCT); and Noordoever Academy, Sint Franciscus Gasthuis, Rotterdam, The Netherlands (JWCT).
Correspondence: Prof. Dr. Jan Willem Cohen Tervaert, Universiteitsingel 40, 6229ER Maastricht, The Netherlands (e-mail: jw.cohentervaert@maastrichtuniversity.nl).
MJK and FV have equally contributed to the work.
The authors report no conflicts of interest.

ISSN: 0025-7974
DOI: 10.1097/MD.0000000000000747

(*Medicine* 94(20):e747)

Abbreviations: AAV = ANCA-associated vasculitis, ANCA = anti-neutrophil cytoplasmic antibodies, FDG = 2-deoxy-2-[^{18}F]-fluoro-D-glucose, PET = positron emission tomography, SUVmax = maximum standard uptake value.

INTRODUCTION

Granulomatosis with polyangiitis (GPA; Wegener's) is an inflammatory disease entity affecting small to medium vessels. It is, together with microscopic polyangiitis (MPA) and eosinophilic granulomatosis with polyangiitis (EGPA; Churg Strauss Syndrome), characterized by the presence of anti-neutrophil cytoplasmic antibodies (ANCA) and they are frequently grouped together under the term ANCA-associated vasculitis (AAV).[1]

Early diagnosis and assessment of the extent of disease activity are important for adequate therapeutic decisions.[1] Multiple tools may be helpful, such as biochemical parameters of inflammation, imaging techniques, and tissue biopsies. Even though these tools suffice to diagnose active disease in most episodes, the results can sometimes be inconclusive. In particular, it is sometimes problematic to determine whether symptoms are due to active disease, vasculitic damage, and/or treatment-related side-effects.

2-deoxy-2-[^{18}F]-fluoro-D-glucose (FDG) positron emission tomography (PET) scanning is used for detecting high glucose metabolism in malignancies, infectious, and auto-immune diseases.[2–4] Co-registration with computed tomography (CT) allows the increased FDG uptake to be localized to the underlying anatomy. PET scanning has been proven to be a useful diagnostic tool in large vessel vasculitis.[5–8] PET scanning can visualize glucose-consuming inflamed vessels, provided that their diameter is >4 mm. The limited spatial resolution was previously thought to be insufficient to detect the involvement of small- and medium-size vessels.[6,7] Recent studies, however, have shown that PET scans show abnormalities in patients with ANCA-associated vasculitis.[9–11] This novel imaging technique may therefore be a useful tool for diagnosing active disease and, in addition, to assess the severity and the extent of the disease. The latter may be relevant to detect occult diagnostic biopsy sites as previously demonstrated in sarcoidosis.[12]

The objective of our study is to explore the ability of PET scanning to assess the extent of disease activity in patients with AAV.

METHODS

Study Population

Consecutive PET scans were performed in patients with AAV at Maastricht University Medical Center (MUMC)

between December 2006 and March 2014 and at Erasme University Hospital (EUH) in Brussels between July 2008 and June 2013 and were retrospectively included. All patients fulfilled a diagnosis of GPA according to the 2012 revised International Chapel Hill Consensus Conference Nomenclature.[13] Patients were previously treated according to the recommendations of the European League Against Rheumatism (EULAR).[14] Disease states were defined according to the EULAR recommendations.[15] A PET scan was performed in patients with clinically suspected disease activity (diagnosis or relapse), whereas other tools for evaluation of activity were inconclusive. The possibility of an active bacterial or viral infection was excluded by culture, serology, and persistence of symptoms despite empirical antibiotic treatment. This study was carried out in compliance with the Helsinki Declaration.

Diagnostic Parameters

An extensive diagnostic work-up was done in all cases, including analysis of clinical features, laboratory assessment, imaging techniques, and, if appropriate, a biopsy. Laboratory assessment included high-sensitivity C-reactive protein (CRP, cutoff value $\geq$10 ng/mL) levels, ANCA levels, and urine analysis at the time of scanning. Hematuria was defined as $\geq$10 erythrocytes in a urinary sediment, combined with dysmorphic erythrocytes and/or red blood cell casts. In Maastricht, ANCA levels were determined using the Fluorescent-Enzyme Immuno-Assay (FEIA) method.[16] FEIA detection for both proteinase-3 (PR3) and myeloperoxidase (MPO) antibodies were fully automated as performed in a UniCAP 100 (Pharmacia Diagnostics). Values $\geq$10 AU were considered positive.

In Brussels, ANCA levels were determined using an enzyme-linked immunosorbent assay (ELISA) method (Euroimmun, Lübeck, Germany) until September 4, 2011. Values >20 U/mL were considered positive. Thereafter, MPO- and PR3-ANCA were detected using a FEIA method in a fully automated Unicap 250 (ThermoFisher Scientific, Waltham, MA). Values of MPO- and PR3-ANCA were considered positive if >5 and >3 IU/mL, respectively.

[^{18}F]-FDG-PET/CT

A whole-body [^{18}F]-FDG-PET/CT scan was performed in both centers. In Maastricht, a Gemini_ PET-CT (Philips Medical Systems) scanner with time-of-flight (TOF) capability was used, together with a 64-slice Brilliance CT scanner. This scanner has a transverse and axial Field of View (FOV) of 57.6 and 18 cm, respectively. The spatial resolution is around 5 mm. In Brussels, a Gemini_ PET-CT (Philips Medical Systems) scanner was used without TOF capability, but with the same PET FOV and spatial resolution, together with a 16-slice Brilliance CT scanner.

Patients were fasting for at least 6 hours before the examination. In all patients, blood glucose was measured to ensure that the blood glucose was <10 mmol/L. The injected total activity of FDG depended on the weight of the patient. Mean injected dose was: 200 MBq. After a resting period of 45 min in Maastricht and 90 min in Brussels (time needed for uptake of FDG), PET and CT images were acquired from the head to the feet. A low-dose CT scan was performed without intravenous contrast agent. The PET images were acquired in 5-min bed positions and were reconstructed using the standard BLOB-OS-TF reconstruction algorithm. PET images were corrected for attenuation, scatter, randoms, dead-time, radioactive decay, and analyzed on a dedicated workstation using a dedicated fusion software (Syntegra, Philips Healthcare). Quantification of FDG uptake was performed by assessing the standardized uptake value (SUV; measured activity concentration [Bq/ml] $\times$ body weight [g]/injected activity [Bq]).

Retrospectively, all PET scans were re-examined by experienced nuclear physicians who were blinded to the clinical symptoms (in Maastricht MvK, SV; in Brussels DB). Findings were scored visually as either positive or negative, in which a positive finding showed non-physiological increased FDG uptake (''hotspot''). Positive PET findings were classified according to their localization. The maximal SUV (SUVmax) was measured at the various PET-positive localizations. PET-positive lesions that were unsuspected based on the clinical evaluation are referred to as ''occult lesions.'' The amount of hotspots and the highest observed SUVmax value were compared during episodes that were ANCA- or CRP-negative versus episodes that were ANCA- or CRP-positive. In these analyses, findings that were related to other causes were excluded.

Statistical Procedure

Numerical variables were expressed as mean (standard deviation) or as median (interquartile range) and categorical variables as numbers (percentages). Gaussian normality was tested with the D'Agostino and Pearson omnibus normality test. Two unpaired variables were compared with the Student unpaired *t* test for parametric data or with the Mann–Whitney test if otherwise. All statistical analyses were performed using GraphPad Prism version 6.04 for Windows (GraphPad Software, La Jolla, CA).

RESULTS

Patient Characteristics

Thirty-three patients were included; an overview of the patient characteristics is shown in Table 1. Twenty patients were positive for PR3-ANCA at diagnosis, 9 patients for MPO-ANCA, and 4 patients were ANCA-negative.

Forty-four PET scans were made during an episode of suspected disease activity (Table 2). Eleven scans were performed at diagnosis and 33 scans at a suspected relapse. The suspected relapses occurred after a median of 68 (30–113) months since diagnosis. In 5 patients, $\geq$2 consecutive episodes occurred during which a PET scan was performed. These patients were in remission between episodes.

Results of PET Scans During Suspected Disease Activity

All PET scans during an episode of suspected disease activity except 2 revealed enhanced non-physiological FDG uptake. Table 3 shows the anatomic location of the positive sites and the corresponding median SUVmax values. The majority of these sites disclosed a SUVmax value between >2.5 and <6. Examples of PET/CT images of patients with AAV are shown in Figures 1 and 2.

Occult Lesions

Forty-one occult lesions were found on the PET scans that were unsuspected based on the clinical evaluations. These lesions were localized in the lung (4 patients), mediastinum (2), nasopharynx (2), parotis (1), orbita (1), skin (3), spleen (2), axillary lymph node (1), cervical lymph node (1), muscles (2),

TABLE 1. Patient Characteristics

Patient Characteristics	All	MUMC	EUH
Patients	33	22	11
PET scans	61	29	32
During suspected activity	44	23	21
During remission	17	6	11
Male	14 (42.4%)	7 (31.8%)	7 (63.6%)
Age	57.1 (15.8)	58.3 (16.5)	54.7 (14.7)
ANCA serotype			
PR3	20 (60.6%)	14 (63.6%)	6 (54.5%)
MPO	9 (27.3%)	5 (22.7%)	4 (36.4%)
Negative	4 (20%)	3 (13.6%)	1 (9.1%)

ANCA = anti-neutrophil cytoplasmic antibodies, MPO = myeloperoxidase, PET = positron emission tomography, PR3 = proteinase 3.

bone marrow (7), aorta (8), thyroid (3), spinal canal (1), kidney (1), skull (1), and pineal gland (1).

Three biopsies were performed after the finding of an occult lesion. In 1 patient, a fine-needle aspiration of the thyroid was performed showing an inflammatory process with giant cells, suggestive of active GPA. A muscle biopsy in another patient revealed a cryptococcal myositis. Lastly, a biopsy of the parotis was suggestive of a Warthin tumor.

TABLE 2. Clinical Characteristics, Biochemical Parameters, and Treatment at PET Scans Made During an Episode of Clinically Suspected Disease Activity

PET Scan Characteristics	All	MUMC	EUH
PET scans	44	23	21
Suspected organ involvement			
Constitutional	21 (47.7%)	9 (39.1%)	12 (57.1%)
Ear, nose, throat	27 (61.4%)	16 (69.6%)	11 (52.4%)
Orbita	5 (11.4%)	5 (21.7%)	0 (0%)
Cutis	6 (13.6%)	4 (17.4%)	2 (9.5%)
Lung	19 (43.2%)	13 (56.5%)	6 (28.6%)
Cardiovascular	1 (2.3%)	1 (4.3%)	0 (0%)
Gastrointestinal	0 (0%)	0 (0%)	1 (4.8%)
Kidney	7 (15.9%)	5 (21.7%)	2 (9.5%)
Nervous system	6 (13.6%)	3 (13.1%)	3 (14.3%)
Laboratorium results			
CRP-positive	21 (47.7%)	12 (52.2%)	9 (42.9%)
ANCA-positive	19 (43.2%)	12 (52.2%)	7 (33.3%)
CRP- and ANCA-positive	11 (25%)	8 (34.8%)	3 (14.3%)
Treatment at the time of scanning			
Prednisone	22 (50%)	16 (69.6%)	12 (57.1%)
Prednisone dosage	15 (6–30)	15 (5–30)	14 (8–28)
Cyclophosphamide	7 (15.9%)	4 (17.4%)	3 (14.3%)
Rituximab	2 (4.5%)	1 (4.3%)	1 (4.8%)
Mofetil mycophenolate	1 (2.3%)	1 (4.3%)	0 (0%)
Methotrexate	9 (20.5%)	1 (4.3%)	8 (38.1%)
Azathioprine	2 (4.5%)	4 (17.4%)	2 (9.5%)

ANCA = anti-neutrophil cytoplasmic antibodies, CRP = C-reactive protein, PET = positron emission tomography.

PET Findings in Relation to CRP and ANCA Positivity

An average of 2.4 (1.5) PET-positive findings were observed during episodes of suspected disease activity (Figure 3). More hotspots were observed during episodes in which the CRP level was elevated ($P = 0.003$). A similar amount of hotspots were observed during episodes in which a positive ANCA was found compared with episodes in which the ANCA level was negative ($P = 0.125$).

The highest observed SUVmax value during the episodes was a median of 5.4 (3.9–7.1). No differences in the highest SUVmax value were observed between episodes with elevated CRP levels and episodes in which CRP levels were not increased ($P = 0.148$). The highest observed SUVmax value tended to be higher during episodes in which the ANCA level was negative, but this did not reach significance ($P = 0.051$, Figure 4).

Follow-Up

Three patients developed additional symptoms after scanning. In two patients, hematuria occurred after the PET scan was made. A kidney biopsy disclosed pauci-immune necrotizing crescentic glomerulonephritis in both. One patient developed nasal mucosal inflammation with bloody discharge, crusts, nasal obstruction, and epistaxis 2 weeks after scanning; the scan did not reveal enhanced uptake in the nasopharynx.

Immunosuppressive treatment was initiated or increased in 37 of 42 (88.1%) episodes with positive findings on the PET scan. In 1 patient, antifungal treatment was initiated after the finding of a fungal infection. In 4 patients, the relapse was treated with cotrimoxazol monotherapy because of a clinically suspected loco-regional relapse with PET-positive findings limited to the respiratory tract.

In 1 patient with a negative PET scan, prednisone (30 mg) was added to the therapy because of persistent symptoms in the nasopharynx. The other patient with a negative PET scan had constitutional symptoms, low-grade fever, arthralgia, and developed symptoms in the nasopharynx 2 weeks after scanning, after which immunosuppressive treatment was subsequently started.

Patients entered remission in 43 of 44 (97.8%) episodes after initiation of treatment. One patient with severe disease developed a partial remission during therapy and died after 4 month due to respiratory insufficiency; at autopsy, a fungal infection was found, possibly secondary to the prolonged immunosuppressive therapy.

A follow-up PET scan was made in 13 episodes after a mean follow-up time of 7 (2.5) months. In 2 patients, 3 follow-up scans were made. The results of the follow-up PET scans are shown in Table 4 (for an example, see Figure 2). On all follow-up scans, SUVmax values normalized to physiological uptake or declined. New localization of enhanced FDG uptake was seen in 3 patients: in 1 patient in the thyroid after 7 months (SUVmax 7.3), in 1 patient in the skull after 9 months (SUVmax 4.7), and in 1 patient in a mediastinal lymph node (SUVmax 16.0).

DISCUSSION

In our study, PET scans in AAV patients revealed positive findings in multiple sites of the body, including sites not

TABLE 3. PET-positive Findings on the PET Scans Made During 36 Episodes of Suspected Disease Activity in 25 Patients With ANCA-associated Vasculitis

	Total		MUMC			EUH		
Anatomic site	**Pt**	**Scans**	**Pt**	**Scans**	**SUVmax**	**Pt**	**Scans**	**SUVmax**
Thoracic	19	25	14	14		5	11	
Mediastinum	12	12	9	9	3.9 (2.8–5.8)	3	3	3.0 (2.6–11.0)
Lung	16	22	11	11	4.7 (3.9–6.3)	5	11	3.9 (1.8–5.2)
Extra thoracic	28	37	18	19		10	18	
Spleen	2	2	2	2	1.5; 2.4	0	0	
Nasopharynx	18	22	13	14	4.1 (3.4–5.4)	5	8	7.1 (4.8–7.2)
Subglottis	2	2	2	2	3.9; 4.7	0	0	
Orbita	3	3	3	3	6.4 (3.9–7.6)	0	0	
Cutaneous	4	4	4	4	4.4 (4.0–5.3)	0	0	
Muscles	2	2	1	1	8.4	1	1	2.7
Axillary lymph node	1	1	1	1	1.6	0	0	
Cervical lymph node	1	1	1	1	4.2	0	0	
Bone marrow	7	8	6	6	2.9 (2.6–3.5)	1	2	2.7; 3.4
Aorta	8	11	4	4	2.9 (1.9–3.4)	4	7	4.7 (3.8–7.6)
Joints	10	11	7	7	2.2 (1.7–2.6)	3	4	2.4 (1.7–3.2)
Thyroid	3	4	3	4	3.1 (2.5–4.7)	0	0	
Pineal gland	1	1	1	1	4.9	0	0	
Kidney	1	2	0	0		1	2	18.4; 25.3
Spinal canal	1	3	0	0		1	3	5.9 (4.7–7.9)
Parotis	1	1	1	1	1.6	0	0	

ANCA = anti-neutrophil cytoplasmic antibodies, PET = positron emission tomography, Pt = patients, SUVmax = maximum standard uptake values.

clinically suspected and difficult to assess otherwise. PET scans may show FDG-positive findings during episodes in which other tools for evaluation of disease activity are inconclusive.

Similar to our findings using Gallium-67 [^{67}Ga] scintigraphy[17] in patients with GPA, PET scans seem to be a sensitive tool to assess disease activity. In our current study, all but 2 scans showed non-physiological FDG uptake during an episode of clinically suspected disease activity. Compared with gallium scanning, however, PET scanning offers additional information. First, Gallium scintigraphy suffers from practical limitations, such as the required interval between time of injection of the radiopharmaceuticals and time of scanning (48–72 hours) and the high radiation exposure. Second, the spatial resolution is higher in PET scans. Third, a low-dose CT scan may be used concomitantly to correlate the FDG uptake with the precise anatomical location. In sarcoidosis, PET scans are of value in detecting occult diagnostic biopsy sites.[12] In our cohort, 41 clinically occult sites were found on the PET scan, and in 1 patient this resulted in a diagnostic biopsy.[9]

Whether hotspots on the PET scan can be attributed to activity of vasculitis is sometimes difficult to assess. A biopsy of PET-positive lesions would result in a definitive diagnosis. However, such a strategy is not realistic, as it does not correspond to routine clinical practice and was not performed in the current study. As we observed a favorable outcome after intensifying immunosuppressive treatment, we hypothesize that these patients indeed had active disease at the time of scanning. It is important to note that PET scans do not differentiate active vasculitis from infections, as observed in 2 of our patients with PET-positive findings due to an underlying fungal infection. In one of these patients, a biopsy of a clinically occult lesion led to the discovery of cryptococcal myositis and masquerading vasculitis.[18] The differentiation between infections and ANCA-mediated disease activity remains an area of uncertainty, especially because there is strong evidence that infections may be an important trigger in the multifactorial etiology of ANCA-associated vasculitis.[19] In the future, more sensitive diagnostic modalities, such as the combination of PET scanning with magnetic resonance imaging (PET/MRI), may identify the infectious foci, which started the cascade leading to the (re)activation of vasculitis.

Most importantly, PET scans revealed abnormalities during episodes of active disease in which ANCA were sometimes not detected and CRP levels not increased. However, more hotspots were observed if the CRP levels were elevated. In contrast, the highest observed SUVmax values were not related to CRP levels. These findings suggest that the disease may be more extensive, but not more severe, if biochemical parameters of inflammation are increased.

Remarkably, multiple hotspots were found in organs that were not clinically suspected, such as the thyroid gland (5 scans in 4 patients), the aorta (11 scans in 8 patients), and bone marrow (8 scans in 7 patients). Stone et al[20] previously reported a high prevalence of thyroid dysfunction in patients with severe AAV. Interestingly, in 4 patients, enhanced uptake was found in the thyroid gland, whereas only 1 patient presented with clinically evident hyperthyroidism.[9] In a case–control study, it was shown that thyroid disease was associated with AAV independently from the use of anti-thyroid agents.[21] Enhanced uptake in the thyroid was seen in 4 scans made during suspected disease activity and in 1 scan during remission. Importantly, none of our current patients suffered from antithyroid drug-associated AAV. The significantly enhanced uptake in the aorta observed in 8 of our patients strongly suggests inflammation of the vessel

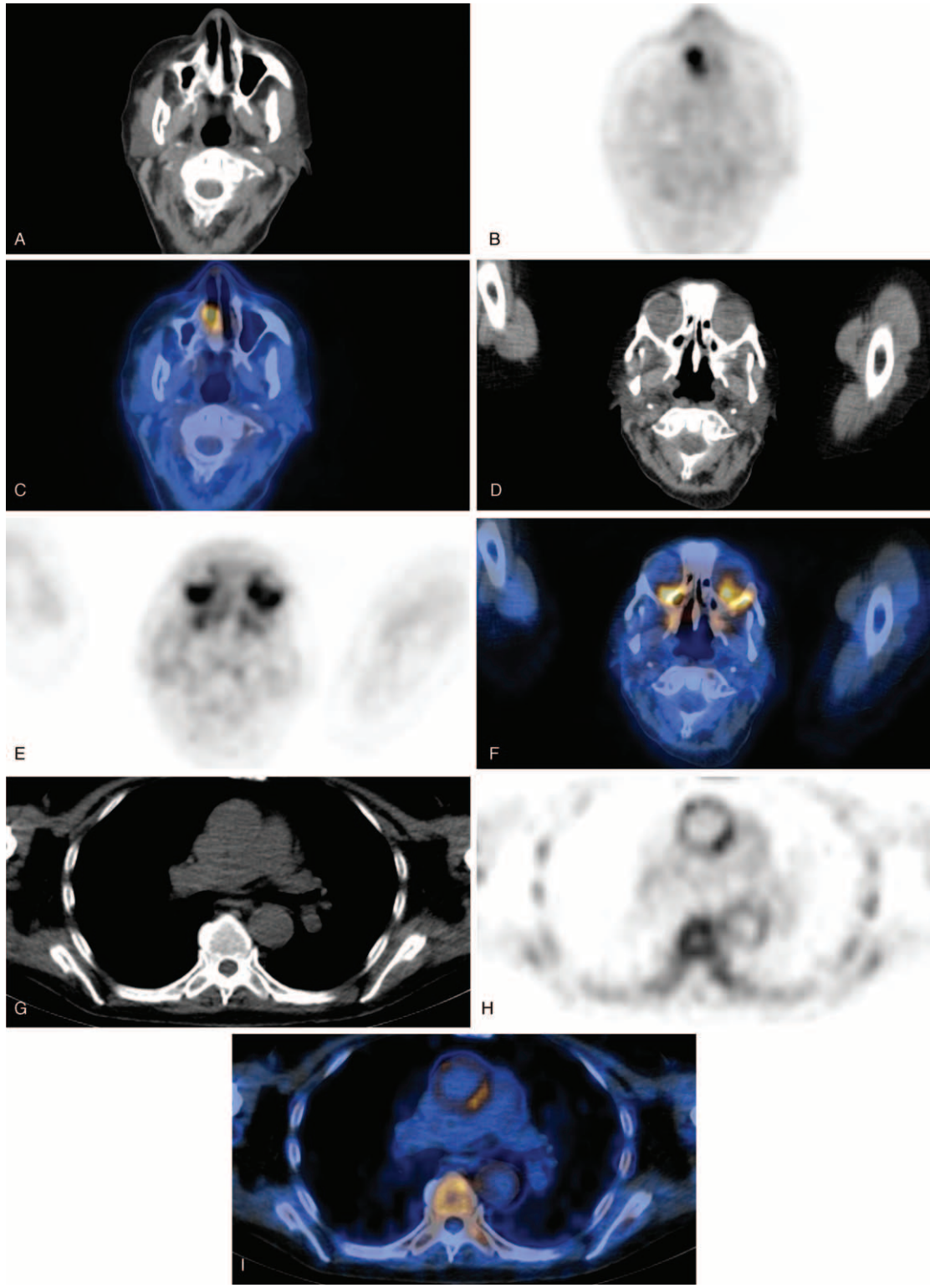

FIGURE 1. Examples of fusion PET/CT images of AAV patients during a period of suspected active disease. (A) CT scan, (B) PET scan, and (C) fusion PET/CT of a patient with suspected nasal involvement. (D) CT scan, (e) PET scan, and (F) fusion PET/CT of a patient with suspected ocular involvement. (G) CT scan, (H) PET scan, and (I) fusion PET/CT of a patient with enhanced uptake in the aorta and bone/bone marrow (occult lesions). (J) CT scan, (K) PET scan, and (L) fusion PET/CT of a patient with aortitis and cervical pachymeningitis (occult lesions). AAV = anti-neutrophil cytoplasmic antibodies-associated vasculitis, CT = computed tomography, PET = positron emission tomography.

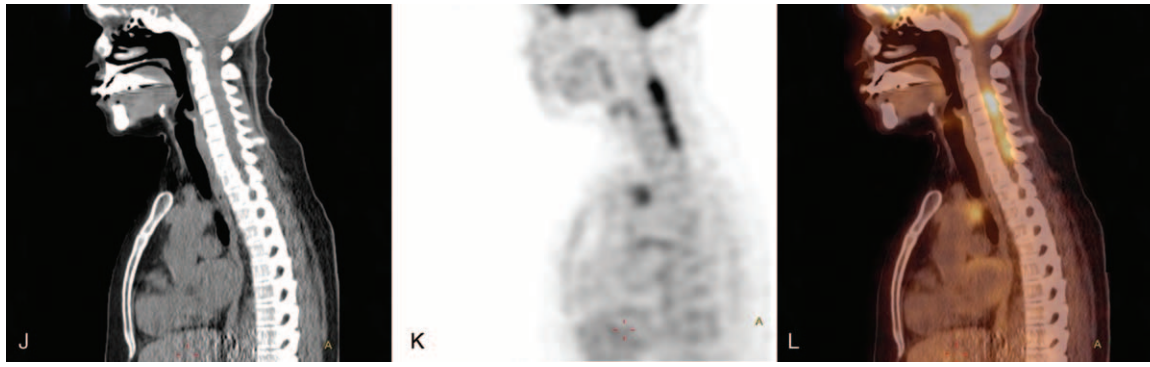

FIGURE 1. (Continued)

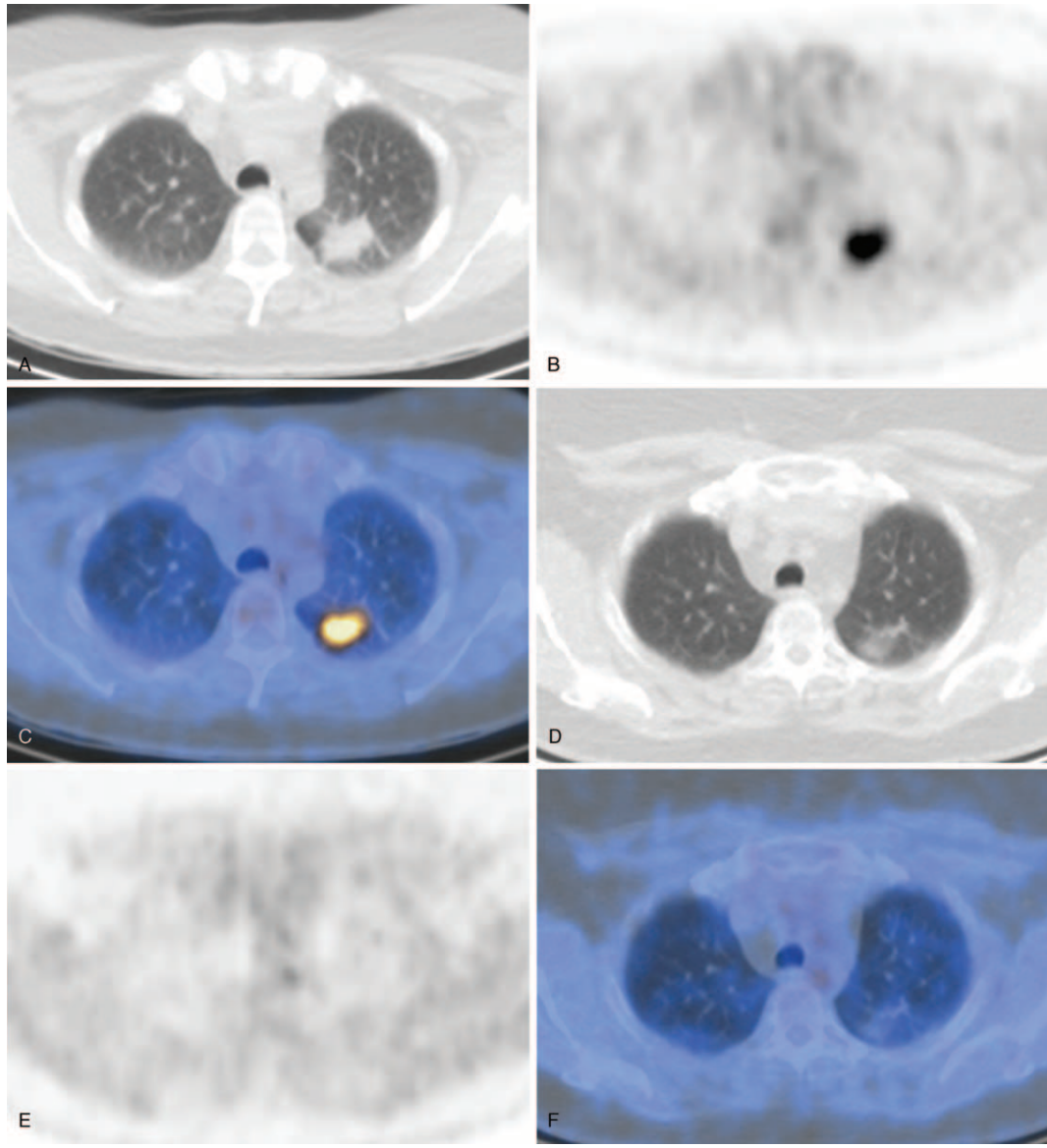

FIGURE 2. Examples of fusion PET/CT images of AAV patients during follow-up. (A) CT scan, (B) PET scan, and (C) fusion PET/CT of a patient with suspected pulmonary disease activity. (d) CT scan, (E) PET scan, and (F) fusion PET/CT of the same patient 5 months later after intensified immunosuppressive treatment. AAV = anti-neutrophil cytoplasmic antibodies-associated vasculitis, CT = computed tomography, PET = positron emission tomography.

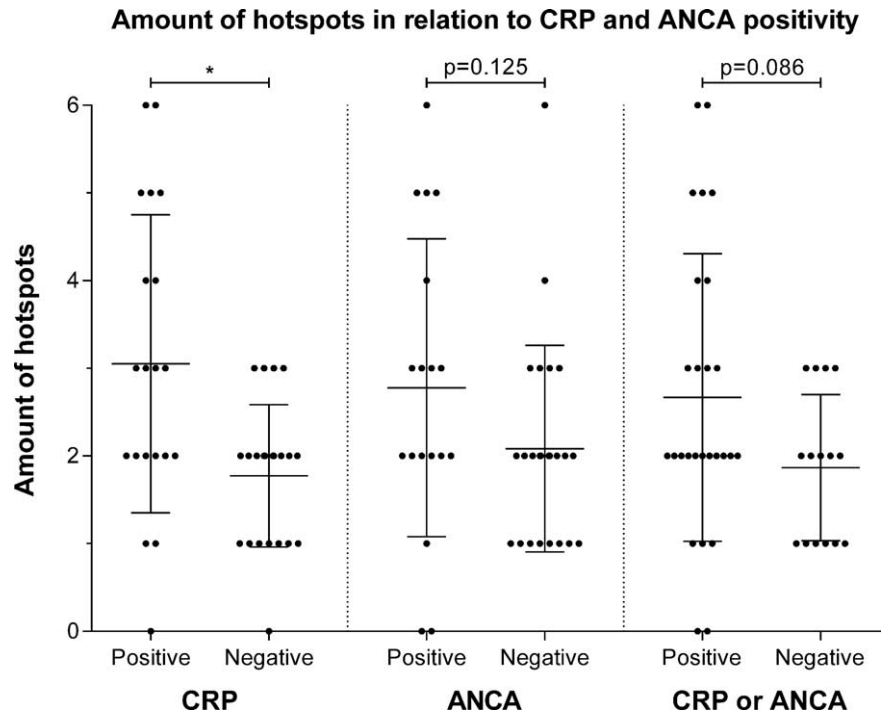

FIGURE 3. Differences in the amount of PET-positive findings observed during episodes that are CRP or ANCA negative compared to CRP (cutoff value ≥10 ng/mL) or ANCA positive episodes. Midline and brackets represent the mean and SD. *$p < 0.01$. ANCA = anti-neutrophil cytoplasmic antibodies, CRP = C-reactive protein, PET = positron emission tomography, SD = standard deviation.

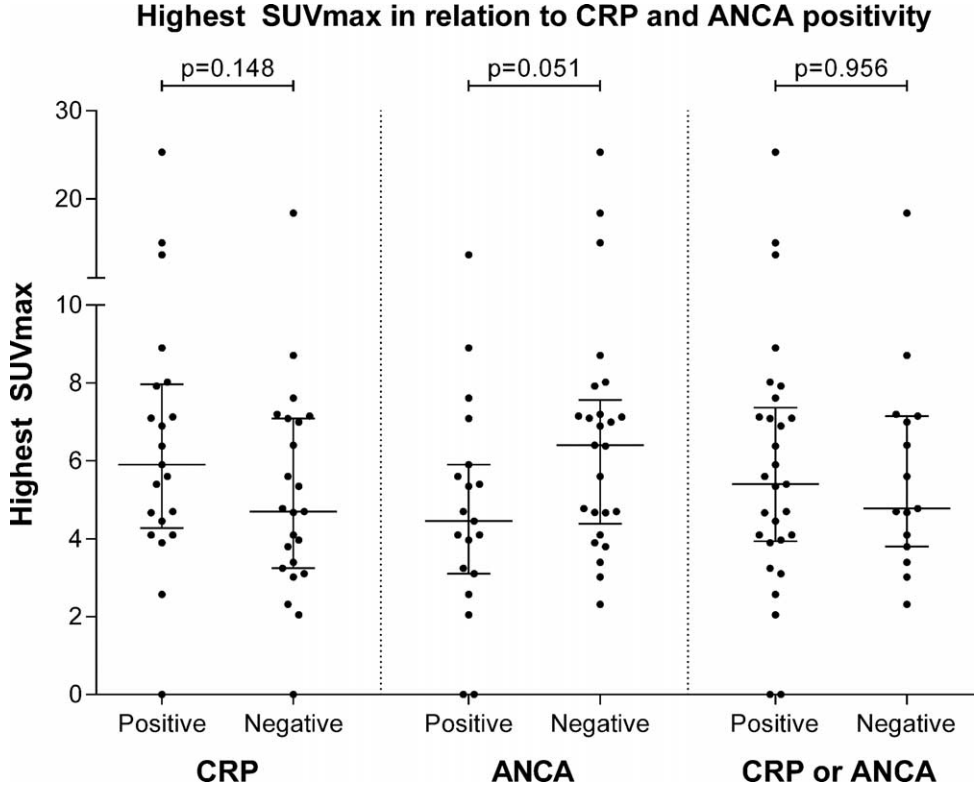

FIGURE 4. Differences in the highest SUVmax value observed during episodes that are CRP- or ANCA-negative compared with CRP (cutoff value ≥10 ng/mL) or ANCA-positive episodes. Midline and brackets represent the median and interquartile range. ANCA = anti-neutrophil cytoplasmic antibodies, CRP = C-reactive protein, SUVmax = maximum standard uptake values.

TABLE 4. Results of the PET Scans Made During Follow-up. In Patient 16, 3 Follow-up Scans Were Performed. In Patient 18, 3 Scans Were Performed During Different Episodes of Suspected Disease Activity and 5 Scans During Follow-up

Pt nr/ Sex/Age	Scan During Disease Activity Organ Involvement (SUVmax)	Treatment Change	Follow-up Scans Organ Involvement (SUVmax)
4/F/52.4	ENT (4.1), thyroid (3.5)	GC, CYC	Mo 9: normalized
7/F/48.6	L (8.9), ENT (6.5), pineal gland (4.9), thyroid (2.4)	GC, CYC	Mo 5: normalized
10/M/72.8	S (3.9), BM (3.5), aorta (1.7), joints (4.7)	GC, RTX, IVIG	Mo 3: BM (3.2), aorta (1.8) joints (3.0)
13/M/71.0	L (4.7)	Sat	Mo 7: thyroid (7.3)
15/M/50.9	ENT (4.5), maxillary sinus (7.1), aorta (3.8)	GC, CYC	Mo 8: ENT (3.1), max (1.2), aorta (1.9)
16/M/63.1	Med (11.0), L (5.2), aorta (13.7)	GC, MTX, RTX	Mo 7: med (5.0), L (4.1), aorta (3.3) Mo 16: med (2.8), L (1.7) Mo 26: L (2.8)
17/F/62.2	ENT (2.1), BM (2.7), aorta (6.4), spinal canal (5.9)	GC, CYC	Mo 6: normalized
18.1/M/39.0	L (6.4), kidney (25.3)	GC, CYC	Mo 5: normalized
18.2/M/40.0	Kidney (18.4)	CYC	Mo 5: kidney (4.3) Mo 10: normalized Mo 18: normalized
18.3/M/42.9	Med (3.0), L (1.6), joints (1.5)	GC, RTX	Mo 9: skull (4.7)
21/M/52.6	L (3.2), muscles (2.7)	GC, CYC	Mo 5: normalized
27/F/24.9	Subglottis (4.7)	Sat, GC, RTX	Mo 8: subglottis (2.6), Med (16.0)
31/F/52.8	Med (15.0), L (2.5), LN C (4.3), S (5.5), muscles (8.4), BM (3.5)	Antifungal	Mo 12: L (2.4)

BM = bone marrow, CYC = cyclophosphamide, ENT = ear, nose and throat, GC = glucocorticoid treatment, IVIG = intravenous immunoglobulin, K = kidney, L = lung, LN C = cervical lymph node, Med = mediastinal, MTX = methotrexate, RTX = rituximab, S = skin, Sat = cotrimoxazol.

wall according to the visual arteritis score as proposed by Meller at al.[22] In all our cases, aortic hypermetabolism was not associated with any obvious clinical impact. Asymptomatic aortic involvement has already been reported in a case series of patients with AAV, but only in 2 patients with EGPA and not in patients with GPA.[23] Notably, in 1 case of the present series, the occurrence of a subclavian murmur raised the question of an overlap between GPA and Takayasu arteritis.[24] The finding of aortic involvement in our series of patients with AAV supports the concept that small-vessel vasculitis may also affect larger vessels.[13] Regarding the evaluation of aortic involvement associated with AAV, PET/MRI has the potential to offer not only a sensitive estimation of inflammatory processes, but also a detailed morphological analysis, which enables exact co-registration and contributes to the differential diagnosis of inflammatory aortic diseases. Pathologically enhanced uptake in the bone marrow is possibly related to chronic stimulation and is in line with the study by Dale et al[25] who found an increased turnover rate of the bone marrow during active disease. These findings of hotspots in clinically unsuspected organs indicate that the disease may be more extensive than previously suspected.[26] The clinical importance of these findings (eg, the prognostic value and therapeutic consequence) is, however, uncertain and should be further investigated.

A PET scan was made in remission during 13 episodes and showed normalized or decreased FDG uptake. These findings suggest a role for PET scanning during follow-up to guide treatment in patients with AAV. The application of PET scanning to monitor disease activity in large vessel vasculitis during immunosuppressive treatment is, however, controversial because steroid administration may hinder the uptake of FDG in the inflammatory lesions.[27,28]

Our study suffers from several limitations. A PET scan was made only in patients difficult to assess, which resulted in a small and highly selected study population. Furthermore, many patients were treated at the time of scanning. Also, few PET scans were made in patients during follow-up. We did not compare our findings using the [^{18}F]-FDG-PET/CT with other imaging modalities, which may provide additional information in conjunction with the PET scan. In addition, we did not compare the results of [^{18}F]-FDG with other radionuclear tracers. In particular, it has been demonstrated that PET scanning with the [^{11}C]-PK11195 can distinguish symptomatic from asymptomatic patients with large vessel vasculitis.[29] Finally, the retrospective design of the study should be taken into account regarding the fact that some hotpots were considered as unexpected on the basis of clinical findings. The strength of our study is that it represents the largest published cohort of patients with AAV in whom a PET scan is made, although the amount of included patients remains limited.

In summary, our study adds to the growing body of data showing that PET scans in patients with AAV reveal FDG-enhanced lesions during disease activity.[9–11] We demonstrated that PET scanning in AAV may show hotspots during an episode of clinically suspected disease activity even when biochemical parameters are inconclusive. In addition, hotspots were found in sites not clinically suspected and difficult to assess otherwise. We hypothesize that a PET scan may be useful to reveal occult biopsy sites if all other tools for evaluation of disease activity are inconclusive. Prospective research is warranted to assess the accuracy of PET scanning in diagnosing and/or monitoring active disease in patients with AAV.

CONCLUSION

PET scans in AAV patients with active disease show positive findings in multiple sites of the body even when biochemical parameters are inconclusive, including sites clinically unsuspected and difficult to assess otherwise.

ACKNOWLEDGMENTS

We would like to thank Mr Salim Anthony Joly for his valuable contribution in the collection of data for the manuscript.

REFERENCES

1. Wilde B, van Paassen P, Witzke O, et al. New pathophysiological insights and treatment of ANCA-associated vasculitis. *Kidney Int.* 2011;79:599–612.
2. Gotthardt M, Bleeker-Rovers CP, Boerman OC, et al. Imaging of Inflammation by PET, conventional scintigraphy, and other imaging techniques. *J Nucl Med.* 2010;51:1937–1949.
3. Mostard RLM, Vöö S, van Kroonenburgh MJPG, et al. Inflammatory activity assessment by F18 FDG-PET/CT in persistent symptomatic sarcoidosis. *Respir Med.* 2011;105:1917–1924.
4. Fletcher JW, Djulbegovic B, Soares HP, et al. Recommendations on the use of 18F-FDG PET in oncology, Journal of nuclear medicine: official publication. *Soc Nucl Med.* 2008;49:480–508.
5. Fuchs M, Briel M, Daikeler T, et al. The impact of 18F-FDG PET on the management of patients with suspected large vessel vasculitis. *Eur J Nucl Med Mol Imag.* 2012;39:344–353.
6. Zerizer I, Tan K, Khan S, et al. Role of FDG-PET and PET/CT in the diagnosis and management of vasculitis. *Eur J Radiol.* 2010;73:504–509.
7. Treglia G, Mattoli M, Leccisotti L, et al. Usefulness of whole-body fluorine-18-fluorodeoxyglucose positron emission tomography in patients with large-vessel vasculitis: a systematic review. *Clin Rheumatol.* 2011;30:1265–1275.
8. Blockmans D, Ceuninck Ld, Vanderschueren S, et al. Repetitive 18F-fluorodeoxyglucose positron emission tomography in giant cell arteritis: A prospective study of 35 patients. *Arthritis Care Res.* 2006;55:131–137.
9. Durme C, Kisters J, Paassen P, et al. Multiple endocrine abnormalities. *Lancet.* 2011;378:540.
10. Ito K, Minamimoto R, Yamashita H, et al. Evaluation of Wegener's granulomatosis using 18F-fluorodeoxyglucose positron emission tomography/computed tomography. *Ann Nucl Med.* 2013;27:209–216.
11. Soussan M, Abisror N, Abad S, et al. FDG-PET/CT in patients with ANCA-associated vasculitis: case-series and literature review. *Autoimmun Rev.* 2014;13:125–131.
12. Teirstein A, Machac J, Almeida O, et al. Results of 188 whole-body fluorodeoxyglucose positron emission tomography scans in 137 patients with sarcoidosis. *Chest.* 2007;132:1949–1953.
13. Jennette JC, Falk RJ, Bacon PA, et al. 2012 revised International Chapel Hill Consensus Conference Nomenclature of Vasculitides. *Arthritis Rheum.* 2013;65:1–11.
14. Mukhtyar C, Guillevin L, Cid MC, et al. EULAR recommendations for the management of primary small and medium vessel vasculitis. *Ann Rheum Dis.* 2009;68:310–317.
15. Hellmich B, Flossmann O, Gross WL, et al. EULAR recommendations for conducting clinical studies and/or clinical trials in systemic vasculitis: focus on anti-neutrophil cytoplasm antibody-associated vasculitis. *Ann Rheum Dis.* 2007;66:605–617.
16. Damoiseaux JGMC, Slot MC, Vaessen M, et al. Evaluation of a new fluorescent-enzyme immuno-assay for diagnosis and follow-up of ANCA-associated vasculitis. *J Clin Immunol.* 2005;25:202–208.
17. Jager R, Poot L, Piers D, et al. Clinical value of gallium-67 scintigraphy in assessment of disease activity in Wegener's granulomatosis. *Ann Rheum Dis.* 2003;62:659–662.
18. Gave AA, Torres R, Kaplan L. Cryptococcal myositis and vasculitis: an unusual necrotizing soft tissue infection. *Surg Infect.* 2004;5:309–313.
19. Konstantinov KN, Ulff-Møller CJ, Tzamaloukas AH. Infections and antineutrophil cytoplasmic antibodies: triggering mechanisms. *Autoimmun Rev.* 2015;14:201–203.
20. Stone JH. Limited versus severe Wegener's granulomatosis: baseline data on patients in the Wegener's granulomatosis etanercept trial. *Arthritis Rheum.* 2003;48:2299–2309.
21. Lionaki S, Hogan SL, Falk RJ, et al. Association between thyroid disease and its treatment with ANCA small-vessel vasculitis: a case-control study. *Nephrol Dial Transplant.* 2007;22:3508–3515.
22. Meller J, Strutz F, Siefker U, et al. Early diagnosis and follow-up of aortitis with [(18)F]FDG PET and MRI. *Eur J Nucl Med Mol Imag.* 2003;30:730–736.
23. Soussan M, Abad S, Mekinian A, et al. Detection of asymptomatic aortic involvement in ANCA-associated vasculitis using FDG PET/CT. *Clin Exp Rheumatol.* 2013;31:S56–S58.
24. Vandergheynst F, Goldman S, Cogan E. Wegener's granulomatosis overlapping with Takayasu's arteritis revealed by FDG-PET scan. *Eur J Intern Med.* 2007;18:148–149.
25. Dale DC, Fauci AS, Wolff SM. The effect of cyclophosphamide on leukocyte kinetics and susceptibility to infection in patients with wegener's granulomatosis. *Arthritis Rheum.* 1973;16:657–664.
26. Kemna MJ, Tervaert JWC. Does one size fit all? *J Rheumatol.* 2013;40:1781–1784.
27. Blockmans D. Diagnosis and extension of giant cell arteritis. Contribution of imaging techniques. *La Presse Médicale.* 2012;41:948–954.
28. Both M, Ahmadi-Simab K, Reuter M, et al. MRI and FDG-PET in the assessment of inflammatory aortic arch syndrome in complicated courses of giant cell arteritis. *Ann Rheum Dis.* 2008;67:1030–1033.
29. Pugliese F, Gaemperli O, Kinderlerer AR, et al. Imaging of vascular inflammation with [11C]-PK11195 and positron emission tomography/computed tomography angiography. *J Am Coll Cardiol.* 2010;56:653–661.